Versatility in Phenolate Bonding in Organoaluminum Complexes Containing Mono- and Bis-*ortho*-Chelating Phenolate Ligands. X-ray Structures of Al{OC$_6$H$_2$(CH$_2$NMe$_2$)$_2$-2,6-Me-4}$_3$, Al(Me)$_2${OC$_6$H$_2$(CH$_2$NMe$_2$)$_2$-2,6-Me-4}·*N*-AlMe$_3$, and Al(Me)$_2${OC$_6$H$_2$(CH$_2$NMe$_2$)$_2$-2,6-Me-4}·*N*-AlMe$_3$·*O*-AlMe$_3$

Marinus P. Hogerheide,[†] Maurits Wesseling,[†] Johann T. B. H. Jastrzebski,[†]
Jaap Boersma,[†] Huub Kooijman,[‡] Anthony L. Spek,[‡,§] and Gerard van Koten*,[†]

*Debye Institute, Department of Metal Mediated Synthesis, and Bijvoet Center for
Biomolecular Research, Laboratory of Crystal and Structural Chemistry, Utrecht University,
Padualaan 8, 3584 CH Utrecht, The Netherlands*

The effect of intramolecular coordination on both the structure and the Lewis acidity of aluminum phenolates has been studied. The mono-*ortho*-amino-substituted phenol HOC$_6$H$_4$(CH$_2$NMe$_2$)-2 (**3**) reacts with AlMe$_3$ to produce the substitution products AlMe$_{3-x}$-(OC$_6$H$_4$(CH$_2$NMe$_2$)-2)$_x$ (x = 1 (**1a**), 2 (**1b**), and 3 (**1c**)) and the trimethylaluminum adduct AlMe$_2$(OC$_6$H$_4$(CH$_2$NMe$_2$)-2)·*O*-AlMe$_3$ (**1d**), all in high yield. For the bis-*ortho*-amino-substituted phenol HOC$_6$H$_2$(CH$_2$NMe$_2$)$_2$-2,6-Me-4 (**4**) the substitution products AlMe$_{3-x}$-(OC$_6$H$_2$(CH$_2$NMe$_2$)$_2$-2,6-Me-4)$_x$ (x = 2 (**2b**) and 3 (**2c**)) were obtained, as well as the mono- and bis(trimethylaluminum) adducts AlMe$_2$(OC$_6$H$_2$(CH$_2$NMe$_2$)$_2$-2,6-Me-4)·*N*-AlMe$_3$ (**2d**) and AlMe$_2$(OC$_6$H$_2$(CH$_2$NMe$_2$)$_2$-2,6-Me-4)·*N*-AlMe$_3$·*O*-AlMe$_3$ (**2e**). The mono(phenolate) dimethylaluminum complexes (**1a** and **2a**) easily undergo an inter- (**1a**) or an intramolecular (**2a**) Lewis base induced ligand exchange to give the bis(phenolate) complexes (**1b** and **2b**, respectively) and trimethylaluminum. The aluminum phenolate complexes were characterized by variable-temperature NMR and single-crystal structure determinations (**2c**−**e**). The solid state structure of **2c** contains the aluminum surrounded by two bidentate, *O,N*-bonded, phenolate ligands and one monodentate, *O*-bonded, phenolate ligand in a trigonal bipyramidal coordination geometry, with the oxygen atoms in the trigonal plane and the two coordinating nitrogen atoms in the apical positions. The molecular structure of **2d** contains one AlMe$_2$ moiety which is bidentate, *O,N*-coordinated by the phenolate ligand, in a distorted tetrahedral geometry. The second amino substituent forms a Lewis acid−base complex with a molecule AlMe$_3$, also with a distorted tetrahedral geometry around the aluminum. The structure of **2e** is similar to that of **2d** but contains an additional molecule of AlMe$_3$, which forms a Lewis acid−base complex with a lone pair of the phenolate oxygen atom, resulting in a distorted tetrahedral geometry around the aluminum. NMR spectroscopy shows the solution structures to be closely related to those established in the solid state.

Introduction

Monomeric aluminum phenolate complexes with bulky *ortho*-substituents (^{t}Bu, Ph) have found applications in the stereo- and regioselective activation of carbonyl groups,[1] the reduction of coordinated benzophenone,[2] and transfer of alkyl groups from aluminum to main-group chlorides.[3] The bulky *ortho*-substituents present in the phenolate ligands prevent association, which is normally found for aluminum phenolate complexes with less sterically demanding *ortho*-substituents.[4] Accordingly, the aluminum centers in these complexes have a free—be it sterically restricted—coordination site available, which enables them to act as Lewis acids.[5−8]

(1) (a) Maruoka, K.; Itoh, T; Sakurai, M.; Nonoshita, K.; Yamamoto, H. *J. Am. Chem. Soc.* **1988**, *110*, 3588. (b) Maruoka, K.; Saito, S.; Yamamoto, H. *J. Am. Chem. Soc.* **1992**, *114*, 1089.
(2) Power, M. B.; Nash, J. R.; Healy, M. D.; Barron, A. R. *Organometallics* **1992**, *11*, 1830.

(3) Healy, M. D.; Ziller, J. W.; Barron, A. R. *Organometallics* **1992**, *11*, 3041.
(4) (a) Pasynkiewicz, S.; Starowieyski, K. B.; Skowrońska-Ptasińska, M. *J. Organomet. Chem.* **1973**, *52*, 269. (b) Starowieyski, K. B.; Skowrońska-Ptasińska, M.; Muszyńska, J. *J. Organomet. Chem.* **1978**, *157*, 379. (c) Starowieyski, K. B.; Pasynkiewicz, S.; Skowrońska, M. D. *J. Organomet. Chem.* **1971**, *31*, 149.
(5) (a) Shreve, A. P.; Mulhaupt, R.; Fultz, W.; Calabrese, J.; Robbins, W.; Ittel, S. D. *Organometallics* **1988**, *7*, 409. (b) Healy, M. D.; Barron, A. R. *Angew. Chem., Int. Ed. Engl.* **1992**, *31*(7), 921. (c) Healy, M. D.; Wierda, D. A.; Barron, A. R. *Organometallics* **1988**, *7*, 2543. (d) Starowieyski, K. B.; Pasynkiewicz, S.; Skowrońska-Ptasińska, M. *J. Organomet. Chem.* **1975**, *90*, C43. (e) Maruoka, K.; Nagahara, S.; Yamamoto, H. *J. Am. Chem. Soc.* **1990**, *112*, 6115.
(6) Healy, M. D.; Ziller, J. W.; Barron, A. R. *J. Am. Chem. Soc.* **1990**, *112*, 2949.
(7) Healey, M. D.; Mason, M. R.; Gravelle, P. H.; Bott, S. G.; Barron, A. R. *J. Chem. Soc., Dalton Trans.* **1993**, 441.
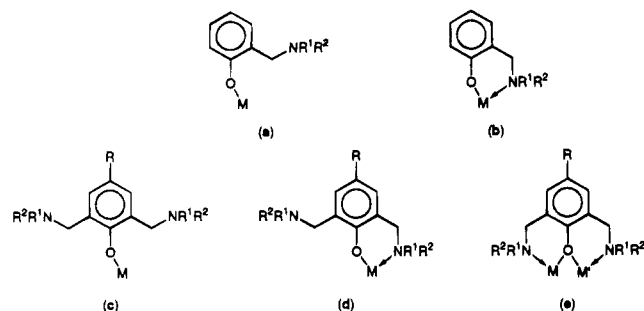
Figure 1. *ortho*-Chelating phenolate ligands and their coordination possibilities: Monodentate (**a, c**), bidentate (**b, d**),[9,10] and bridging between identical (M = M')[11,12] or different (M ≠ M')[13] metal centers (**e**).

The use of phenolates with potentially intramolecularly coordinating *ortho*-substituents provides an attractive alternative to steric bulk. When coordinated, these substituents combine steric shielding of the metal center with electron donation to the metal center. When pendant, they provide steric shielding. For example, the monoanionic 2-[(dimethylamino)methyl]phenolate (see Figure 1a,b) can serve either as an *ortho*-hindered monodentate or as a bidentate ligand, depending on the steric and electronic requirements of the metal center. Introduction of a second *ortho*-amino substituent as in monoanionic 2,6-[(dimethylamino)methyl]-4-methylphenolate (see Figure 1c–e) essentially brings in a second *ortho*-hindering substituent but also another Lewis basic functional group when the ligand coordinates in bidentate fashion, a feature that will be shown to be of importance in the chemistry presented below.

In this paper we report the first results of the systematic study of the effect of *ortho*-chelation on the structure in solution as well as in the solid state and the reactivity of aluminum phenolates.

Experimental Section

General Methods. All reactions were performed in an atmosphere of dry, oxygen-free dinitrogen using standard Schlenk and syringe techniques. All solvents were carefully dried and distilled prior to use. AlMe$_3$ was used as a 2.0 M solution in hexane as obtained from Aldrich. The phenols HOC$_6$H$_4$(CH$_2$NMe$_2$)-2 (**3**) and HOC$_6$H$_2$(CH$_2$NMe$_2$)$_2$-2,6-Me-4 (**4**) were synthesized according to literature procedures.[11] Elemental analyses were performed by H. Kolbe, Mikroanalytisches Laboratorium, Mülheim, Germany. ^{1}H and ^{13}C NMR data were collected on Bruker AC200 and AC300 spectrometers.

AlMe$_2$\{OC$_6$H$_4$(CH$_2$NMe$_2$)-2\} (1a). To a stirred solution of AlMe$_3$ (9.0 mmol; 4.5 mL of a 2.0 M hexane solution) in hexane

(8) For a review on sterically crowded aluminum phenolate complexes see: Healy, M. D.; Power, M. B.; Barron, A. R. *Coord. Chem. Rev.* **1994**, *130*, 63.

(9) van der Schaaf, P. A.; Boersma, J.; Smeets, W. J. J.; Spek, A. L.; van Koten, G. *Inorg. Chem.* **1993**, *32*, 5108.

(10) Alsters, P. L.; Teunissen, H. T.; Boersma, J.; Spek, A. L.; van Koten, G. *Organometallics* **1993**, *12*, 4691.

(11) (a) van der Schaaf, P. A.; Jastrzebski, J. T. B. H.; Hogerheide, M. P.; Smeets, W. J. J; Spek, A. L.; van Koten, G. *Inorg. Chem.*, **1993**, *32*, 4111. (b) Hogerheide, M. P.; Ringelberg, S. N.; Janssen, M. D.; Boersma, J.; Spek, A. L.; van Koten, G. To be published.

(12) (a) van der Schaaf, P. A.; Hogerheide, M. P.; Grove, D. M.; Spek, A. L.; van Koten, G. *Chem. Soc., Chem. Commun.* **1992**, 1703. (b) Tesh, K. F.; Hanusa, T. P. *J. Chem. Soc., Chem. Commun.* **1991**, 879. (c) Gultneh, Y.; Farooq, A.; Liu, S.; Karlin, K. D.; Zubieta, J. *Inorg. Chem.* **1992**, *31*, 3607. (d) Teipel, S.; Griesar, K.; Haase, W.; Krebs, B. *Inorg. Chem.* **1994**, *33*, 456.

(13) Hogerheide, M. P.; Jastrzebski, J. T. B. H.; Boersma, J.; Smeets, W. J. J.; Spek, A. L.; van Koten, G. *Inorg. Chem.* **1994**, *33*, 4431.

(25 mL) a solution of HOC$_6$H$_4$(CH$_2$NMe$_2$)-2 (1.36 g; 9.0 mmol) was added dropwise at 0 °C. While methane gas evolved from the mixture, a white precipitate was formed. After the mixture was stirred for an additional 2 h at room temperature the solvent was removed *in vacuo* and the product washed once with pentane (30 mL). Complex **1a** was obtained as a white powder in quantitative yield. Recrystallization from hexane afforded **1a** as colorless hexagonal crystals. Mp: 125 °C.

^{1}H NMR data (C$_6$D$_6$, 200 MHz, 298 K) (δ)SPCLN 7.13 (m, 2H, Ar*H*); 6.69 (m, 2 H, Ar*H*); 3.05 (s, 2 H, C*H$_2$*N); 1.60 (s, 6 H, N*Me$_2$*); −0.56 (s, 6H, Al*Me$_2$*). ^{13}C NMR data (C$_6$D$_6$, 50 MHz, 298 K) (δ)SPCLN 160.37 (*C*O); 130.89, 129.43, 120.40, 117.23 (Ar); 120.70 (*C*CH$_2$); 62.39 (*C*H$_2$N); 44.33 (N*Me$_2$*). Anal. Calcd for C$_{11}$H$_{18}$NOAl: C, 63.75; H, 8.75; N, 6.76. Found: C, 63.88; H, 8.83; N, 8.82.

AlMe\{OC$_6$H$_4$(CH$_2$NMe$_2$)-2\}$_2$ (1b). The preparation of **1b** was analogous to that of **1a**. Addition of HOC$_6$H$_4$(CH$_2$NMe$_2$)-2 (2.72 g; 18 mmol) to a stirred solution of AlMe$_3$ (4.5 mL; 9.0 mmol) at 0 °C afforded **1b**, after workup, in quantitative yield. Mp: >200 °C.

^{1}H NMR data (C$_6$D$_6$, 200 MHz, 298 K) (δ)SPCLN 7.23 (m, 2 H, Ar*H*); 6.89 (d, 2 H, $^3J_{HH}$ = 7.9 Hz, Ar*H*); 6.80 (m, 4 H, Ar*H*); 3.68 (d, 2 H, $^2J_{HH}$ = 13.5 Hz, C*H$_2$*N); 3.15 (d, 2 H, J_{HH} = 13.5 Hz, C*H$_2$*N); 2.12 (s, 6 H, N*Me$_2$*); 1.98 (s, 6 H, N*Me$_2$*); −0.63 (s, 3 H, Al*Me*). ^{13}C NMR data (C$_6$D$_6$, 50 MHz, 298 K) (δ): 160.16 (*C*O); 129.45, 129.28, 122.96, 119.54, 117.29 (Ar); 62.59 (*C*H$_2$N); 45.69 (N*Me$_2$*). Anal. Calcd for C$_{19}$H$_{27}$N$_2$O$_2$Al: C, 66.65; H, 7.95; N, 8.18. Found: C, 66.20; H, 7.40; N, 8.06.

Al\{OC$_6$H$_4$(CH$_2$NMe$_2$)-2\}$_3$ (1c). The preparation of **1c** was analogous to that of **1a**. Addition of HOC$_6$H$_4$(CH$_2$NMe$_2$)-2 (3.63 g; 24 mmol) to a stirred solution of AlMe$_3$ (4.0 mL; 8.0 mmol) at room temperature afforded **1c** in quantitative yield. Crystallization from hexane at −30 °C resulted in the formation of colorless, hexagonal crystals. Mp: 165 °C (dec).

^{1}H NMR data (C$_6$D$_6$, 200 MHz, 298 K) (δ): 7.38 (d, 1 H, $^3J_{HH}$ = 7.4 Hz, *o*-H); 7.25 (m, 1 H, Ar*H*); 6.96 (m, 3 H, Ar*H*); 6.77 (m, 7 H, Ar*H*); 3.89 (br, 2 H, C*H$_2$*N); 3.53 (d, 1 H, $^2J_{HH}$ = 12.4 Hz, C*H$_2$*N); 3.26 (m, 3 H, C*H$_2$*N); 2.23 (s, 6 H, N*Me$_2$*); 2.14 (s, 6 H, N*Me$_2$*); 2.09 (s, 6 H, N*Me$_2$*). ^{13}C NMR data (C$_6$D$_6$, 50 MHz, 298 K) (δ): 159.73, 159.18 (*C*O); 129.56, 129.15, 128.85, 123.02, 119.62, 117.94, 117.61 (Ar); 62.94, 59.53 (*C*H$_2$N); 46.72, 45.92, 45.57 (N*Me$_2$*). Anal. Calcd for C$_{27}$H$_{36}$N$_3$O$_3$Al: C, 67.90; H, 7.60; N, 8.80. Found: C, 67.75; H, 7.54; N, 8.78.

AlMe$_2$\{OC$_6$H$_4$(CH$_2$NMe$_2$)-2\}·AlMe$_3$ (1d). The preparation of **1d** was analogous to that of **1a**. Addition of HOC$_6$H$_4$(CH$_2$NMe$_2$)-2 (1.97 g; 13 mmol) to a stirred solution of AlMe$_3$ (20 mL; 40 mmol) at 0 °C afforded **1d**, after workup, in quantitative yield. Mp: 90 °C.

^{1}H NMR data (C$_6$D$_6$, 200 MHz, 298 K) (δ): 7.16 (m, 1 H, Ar*H*); 7.00 (m, 1 H, Ar*H*); 6.75 (m, 1 H, Ar*H*); 6.57 (m, 1 H, Ar*H*); 2.98 (s, 2 H, C*H$_2$*N); 1.52 (s, 6 H, N*Me$_2$*); −0.29 (s, 9 H, Al*Me$_3$*); −0.63 (s, 6 H, Al*Me$_2$*). ^{13}C NMR data (C$_6$D$_6$, 50 MHz, 298 K) (δ): 153.17 (*C*O); 131.05, 130.02, 124.72, 124.14, 123.72 (Ar); 61.71 (*C*H$_2$N); 46.58 (N*Me$_2$*); −5.10(Al*Me$_3$*); −9.67 (Al*Me$_2$*). Anal. Calcd for C$_{14}$H$_{27}$NOAl$_2$: C, 60.20; H, 9.74; N, 5.01. Found: C, 60.09; H, 9.70; N, 5.09.

AlMe\{OC$_6$H$_2$(CH$_2$NMe$_2$)$_2$-2,6-Me-4\}$_2$ (2b). The preparation of **2b** was analogous to that of **1a**. Addition of HOC$_6$H$_2$-(CH$_2$NMe$_2$)$_2$-2,6-Me-4 (3.45 g; 15.5 mmol) to a stirred solution of AlMe$_3$ (4.0 mL; 8.0 mmol) at 0 °C resulted in the formation of a slightly yellow, clear solution. Complex **2b** was obtained, after workup, as a yellow powder or oil in essentially quantitative yield. The product contained some unidentified impurities that could not be removed.

^{1}H NMR data (C$_6$D$_6$, 200 MHz, 298 K) (δ): 7.30 (s, 2 H, Ar*H*); 6.58 (s, 2 H, Ar*H*); 3.54 (br, 4 H, C*H$_2$*N); 2.9–1.9 (m, 35 H, C*H$_2$*N, N*Me$_2$*, *p-Me*); −0.57 (s, 3 H, Al*Me$_2$*). ^{13}C NMR data (C$_6$D$_6$, 50 MHz, 298 K) (δ): 156.44 (*C*O); 131.72, 124.89, 122.62 (Ar); 62.80, 60.10 (*C*H$_2$N); 45.72 (N*Me$_2$*); 20.71 (*p-Me*).

Al\{OC$_6$H$_2$(CH$_2$NMe$_2$)$_2$-2,6-Me-4\}$_3$ (2c). After the addition of HOC$_6$H$_2$(CH$_2$NMe$_2$)$_2$-2,6-Me-4 (6.00 g; 27.0 mmol) to a

Table 1. Crystallographic Data for the Complexes 2c–e

	complex		
	2c	**2d**	**2e**
Crystal Data			
formula	$C_{39}H_{63}N_6O_3Al$	$C_{18}H_{36}N_2OAl_2$	$C_{21}H_{45}N_2OAl_3$
M_n	690.97	350.46	422.55
cryst system	monoclinic	orthorhombic	monoclinic
space group	$C2/c$	$Pbca$	$P2_1/c$
a, Å	26.831(2)	12.014(2)	11.5731(17)
b, Å	23.904(3)	15.496(1)	19.893(3)
c, Å	12.9273(16)	24.078(4)	14.5892(13)
β, deg	107.354(9)	90	129.036(11)
V, Å^3	7913.7(16)	4482.6(11)	2608.9(7)
D_{calc}, g cm^{-3}	1.160	1.038	1.076
Z	8	8	4
$F(000)$, e	3008	1536	928
μ, cm^{-1}	0.9	1.3	1.5
cryst size, mm	$0.10 \times 0.23 \times 0.38$	$0.12 \times 0.30 \times 0.60$	$0.70 \times 0.40 \times 0.40$
Data Collection			
T, K	150	150	150
radiation, λ, Å	Mo Kα, 0.170 73 (graphite monochr)	Mo Kα, 0.710 73 (graphite monochr)	Mo Kα, 0.710 73 (graphite monochr)
$\Delta\omega$, deg	$0.60 + 0.35 \tan\theta$	$0.99 + 0.35 \tan\theta$	$0.54 + 0.35 \tan\theta$
hor, ver aperture, mm	3.00, 4.00	2.60, 4.00	3.00, 4.00
ref reflcns	225, 10,2,2 622	241, 225, 062	253, 124, 042
data set, hkl	−34:34, 0:31, −16:16	−15:0, −20:13, −31:0	−15:14, −25:0, −18:18
tot. unique data	9073	5127	5947
obsd data	4358 ($I > 3\sigma(I)$)	2141 ($I > 2\sigma(I)$)	3638 ($I > 2.5\sigma(I)$)
Refinement			
no. of refined params	450	218	285
final R^a	0.064	0.098 [2141 $F > 4\sigma(F)$]	0.0542
final w$R_2{}^b$		0.256	
final $R_w{}^c$	0.050		0.0449
weighting scheme^d	$[\sigma^2(F)]^{-1}$	$[\sigma^2(F) + (0.1136P)^2]^{-1}$	$[\sigma^2(F)]^{-1}$
$(\Delta/\sigma)_{av}$, $(\Delta/\sigma)_{max}$	0.03, 0.7	0.00, 0.011	0.9877, 0.0152
min and max resid density, e Å^{-3}	−0.47, 0.72	−0.45, 0.50	−0.32, 0.33

$^a R = \Sigma||F_o| - |F_c||/\Sigma|F_o|$. $^b wR_2 = [\Sigma[w(F_o^2 - F_c^2)^2]/\Sigma[w(F_o^2)^2]]^{1/2}$. $^c R_w = [\Sigma[w(||F_o| - |F_c||)^2/\Sigma[w(F_o^2)]]^{1/2}$. $^d P = (\max(F_o^2,0) + 2Fc^2)/3$.

stirred solution of AlMe₃ (4.5 mL; 9.0 mmol), the mixture was heated under reflux for 48 h. The usual workup (cf. **1a**), followed by purification of the crude product by recrystallization from toluene, afforded **2c** as a yellow powder in 60–80% yield. Mp: 170 °C (dec).

¹H NMR data (C₆D₆, 200 MHz, 298 K) (δ): 7.42 (s, 2 H, Ar*H*); 7.25 (s, 2 H, Ar*H*); 6.58 (s, 2 H, Ar*H*); 3.65 (br, 2 H, C*H*₂N); 3.47 (br, 6 H, C*H*₂N); 2.6–2.0 (m, 49 H, C*H*₂N, N*Me*₂, *p*-Me). ¹³C NMR data (C₆D₆, 50 MHz, 298 K): δ 156.09 (*CO*); 154.17 (*CO*); 131.69, 130.27, 125.97, 125.44, 122.61 (Ar); 63.71, 60.35, 59.24 (*C*H₂N); 45.86, 45.75 (br, N*Me*₂); 21.10, 20.73 (*p*-Me). Anal. Calcd for C₃₉H₆₃N₆O₃Al: C, 67.80; H, 9.19; N, 12.16. Found: C, 67.77; H, 9.10; N, 12.11.

AlMe₂{OC₆H₂(CH₂NMe₂)₂-2,6-Me-4}·*N*-AlMe₃ (2d). Addition of HOC₆H₂(CH₂NMe₂)₂-2,6-Me-4 (2.22 g; 10.0 mmol) to a stirred solution of 2 molar equiv of AlMe₃ (10 mL; 20 mmol) at 0 °C resulted in the formation of a white precipitate. After the mixture was stirred for an additional 1 h, the product was centrifuged off and dried *in vacuo*. Recrystallization from warm hexane afforded **2d** as a white crystalline solid in 90% yield. Mp: 125 °C.

¹H NMR data (C₆D₆, 300 MHz, 298 K) (δ): 6.72 (s, 1 H, Ar*H*); 6.43 (s, 1 H, Ar*H*); 4.03 (s, 2 H, C*H*₂N); 3.01 (s, 2 H, C*H*₂N); 2.19 (s, 6 H, N*Me*₂); 2.16 (s, 3 H, *p*-Me); 1.58 (s, 6 H, N*Me*₂); −0.31 (s, 9 H, Al*Me*₃); −0.62 (s, 6 H, Al*Me*₂). ¹³C NMR data (C₆D₆, 75 MHz, 298 K) (δ): 157.12 (*CO*); 134.92, 130.62, 125.31 (Ar); 62.24, 54.65 (*C*H₂N); 44.29, 42.83 (N*Me*₂); 20.47 (*p*-Me); −9.18, −11.41 (Al*Me*). Anal. Calcd for C₁₈H₃₆N₂OAl₂: C, 61.69; H, 10.35; N, 7.99. Found: C, 61.54; H, 10.28; N, 7.85.

AlMe₂{OC₆H₂(CH₂NMe₂)₂-2,6-Me-4}·(*N*-AlMe₃)(*O*-Al-Me₃) (2e). The preparation of **2e** was analogous to that of **2d**. Addition of HOC₆H₂(CH₂NMe₂)₂-2,6-Me-4 (2.22 g; 10.0 mmol) to a stirred solution of 4 equiv of AlMe₃ (20 mL; 40 mmol) at 0 °C resulted in the formation of a white precipitate.

Workup afforded **2e** as a white crystalline solid in 92% yield. Mp: 115 °C.

¹H NMR data (C₆D₆, 200 MHz, 298 K) (δ): 6.93 (s, 1 H, Ar*H*); 6.39 (s, 1 H, Ar*H*); 4.14 (s, 2 H, C*H*₂N); 3.03 (s, 2 H, C*H*₂N); 2.23 (s, 6 H, N*Me*₂); 2.13 (s, 3 H, *p*-Me); 1.55 (s, 6 H, N*Me*₂); −0.26 (s, 9 H, Al*Me*₃); −0.35 (s, 9 H, Al*Me*₃); −0.59 (s, 6 H, Al*Me*₂). ¹³C NMR data (C₆D₆, 50 MHz, 298 K) (δ): 153.43 (*CO*); 135.87, 131.40, 130.45, 123.98 (Ar); 62.16, 55.71 (*C*H₂N); 46.04, 43.83 (N*Me*₂); 20.44 (*p*-Me); −5.21, −8.55, −9.23 (Al*Me*). Anal. Calcd for C₂₁H₄₅N₂OAl₃: C, 59.69; H, 10.73; N, 6.63. Found: C, 59.55; H, 10.62; N, 6.67.

X-ray Data Collection and Structure Refinement. Colorless crystals of **2c**–**e** were sampled directly into a viscous oil, glued on top of a glass fiber, and transferred into the cold nitrogen stream on an Enraf-Nonius CAD4T rotating anode diffractometer for data collection. Accurate unit-cell parameters were determined by least squares treatment of 25 well-centered reflections (SET4) in the range 11 < θ < 14°. All data were collected with the $\omega/2\theta$ scan mode. Crystal data and details on data collection and refinement are collected in Table 1. Data were corrected for *Lp* effects, for the observed linear decay of the reference reflections, and for absorption (**2e**, DIFABS;[14] correction range 0.798–1.191). The structures were solved using direct methods (**2c**, SIR92;[15] **2d,e**, SHELXS86[16]) and subsequent difference Fourier techniques. Refinement was carried out by full-matrix least squares techniques on *F* (**2c,e**, SHELX76[17]) or on F^2 (**2d**, SHELXL92).[18]

(14) Walker, N.; Stuart, D. *Acta Crystallogr., Sect. A* **1983**, *39*, 158.
(15) Altomare, A.; Cascarano, G.; Giacovazzo, C.; Guagliardi, A. *J. Appl. Crystallogr.* **1993**, *26*, 343.
(16) Sheldrick, G. M. *SHELXS86. Program for crystal structure determination*; University of Göttingen, Göttingen, Federal Republic of Germany, 1986.

Table 2. Final Coordinates and Equivalent Isotropic Thermal Parameters of the Non-Hydrogen Atoms for 2c

atom	x	y	z	U_{eq},[a] Å^2
Al	0.26480(5)	0.10502(5)	0.77401(10)	0.0187(3)
O(1)	0.32714(9)	0.13085(10)	0.78296(19)	0.0214(9)
O(2)	0.20576(10)	0.14157(10)	0.7566(2)	0.0199(8)
O(3)	0.26228(11)	0.03367(10)	0.7865(2)	0.0258(9)
N(1)	0.27906(12)	0.11772(12)	0.9397(2)	0.0188(10)
N(2)	0.37826(12)	0.21969(14)	0.6703(3)	0.0253(11)
N(3)	0.25081(12)	0.10608(13)	0.6073(2)	0.0200(10)
N(4)	0.11736(12)	0.16686(13)	0.8817(3)	0.0254(11)
N(5)	0.40620(13)	−0.04883(15)	0.8530(3)	0.0360(12)
N(6)[b]	0.11773(18)	−0.0432(2)	0.7135(4)	0.0409(19)
C(1)	0.37168(15)	0.13955(15)	0.8642(3)	0.0211(12)
C(2)	0.37586(15)	0.12513(16)	0.9715(3)	0.0216(12)
C(3)	0.42227(15)	0.13588(16)	1.0520(3)	0.0252(14)
C(4)	0.46515(16)	0.15960(17)	1.0305(3)	0.0275(14)
C(5)	0.46000(15)	0.17233(17)	0.9221(3)	0.0277(14)
C(6)	0.41418(15)	0.16296(16)	0.8394(3)	0.0237(12)
C(7)	0.51530(15)	0.17258(18)	1.1192(3)	0.0388(17)
C(8)	0.41240(15)	0.17347(16)	0.7224(3)	0.0270(14)
C(9)	0.39600(18)	0.27207(17)	0.7262(3)	0.0431(17)
C(10)	0.37809(16)	0.22355(18)	0.5576(3)	0.0344(16)
C(11)	0.33157(14)	0.09550(16)	0.9987(3)	0.0229(12)
C(12)	0.23963(14)	0.08893(16)	0.9802(3)	0.0253(14)
C(13)	0.27764(16)	0.17842(15)	0.9657(3)	0.0574(17)
C(14)	0.16065(15)	0.14410(16)	0.6753(3)	0.0204(12)
C(15)	0.15411(15)	0.11762(16)	0.5754(3)	0.0225(12)
C(16)	0.10652(15)	0.12128(17)	0.4954(3)	0.0276(16)
C(17)	0.06456(15)	0.15015(18)	0.5094(3)	0.0289(14)
C(18)	0.07193(15)	0.17725(17)	0.6081(3)	0.0278(16)
C(19)	0.11895(15)	0.17464(16)	0.6911(3)	0.0216(12)
C(20)	0.01318(15)	0.1542(2)	0.4212(3)	0.0456(19)
C(21)	0.19721(14)	0.08314(16)	0.5540(3)	0.0233(12)
C(22)	0.28808(15)	0.06957(17)	0.5732(3)	0.0290(14)
C(23)	0.25444(15)	0.16374(15)	0.5680(3)	0.0249(14)
C(24)	0.12455(15)	0.20410(16)	0.7973(3)	0.0250(12)
C(25)	0.13006(17)	0.19588(17)	0.9858(3)	0.0363(17)
C(26)	0.06367(15)	0.14712(18)	0.8527(3)	0.0397(17)
C(27)	0.26263(16)	−0.02211(15)	0.7798(3)	0.0206(11)
C(28)	0.21558(15)	−0.05146(17)	0.7690(3)	0.0227(14)
C(29)	0.21592(16)	−0.10918(17)	0.7655(3)	0.0270(16)
C(30)	0.26113(18)	−0.13938(15)	0.7726(3)	0.0263(14)
C(31)	0.30689(16)	−0.10975(17)	0.7837(3)	0.0253(14)
C(32)	0.30845(15)	−0.05169(16)	0.7864(3)	0.0205(14)
C(33)	0.26034(18)	−0.20283(15)	0.7695(3)	0.0401(16)
C(34)	0.35825(14)	−0.02031(16)	0.7940(3)	0.0271(12)
C(35)	0.41109(17)	−0.0519(2)	0.9682(3)	0.0501(19)
C(36)	0.45137(17)	−0.0192(2)	0.8376(4)	0.054(2)
C(37)	0.16719(14)	−0.01929(19)	0.7690(3)	0.0357(16)
C(38)	0.11145(18)	−0.0440(2)	0.5939(4)	0.056(2)
C(39)[b]	0.0758(2)	−0.0096(3)	0.7330(5)	0.067(3)

[a] U(eq) = $^1/_3$ of the trace of the orthogonalized **U**. [b] Major disorder form (77%).

Hydrogen atoms were introduced on calculated positions (C–H = 0.98 Å) and included in the refinement riding on their carrier atoms. All non-hydrogen atoms were refined with anisotropic thermal parameters. The structure determination for **2c** showed some disorder in the positions of N(6) and C(39), which was modeled and refined using fractional site occupation factors and anisotropic thermal parameters for the major positions only. The hydrogen atoms of **2d** were refined with a fixed isotropic thermal parameter related to the value of the equiv isotropic thermal parameter of their carrier atoms by a factor of 1.5 for the methyl hydrogen atoms and by a factor of 1.2 for the other hydrogen atoms. Weights were introduced in the last refinement cycles. Positional parameters are listed in Tables 2–4 for **2c–e**, respectively. Neutral atom scattering factors were taken from Cromer and Mann[19] and corrected for anomalous dispersion[20] for **2c,e**. Neutral atom scattering factors and anomalous dispersion corrections were taken from

(17) Sheldrick, G. M. *SHELX76. Crystal structure analysis package*; University of Cambridge: Cambridge, England, 1976.
(18) Sheldrick, G. M. *SHELXL-93. Program for crystal structure refinement,*; University of Göttingen: Göttingen, Germany, 1993.

Table 3. Final Coordinates and Equivalent Isotropic Thermal Parameters of the Non-Hydrogen Atoms for 2d

atom	x	y	z	U_{eq},[a] Å^2
Al(1)	0.35656(12)	0.18802(10)	0.28920(6)	0.0281(5)
Al(2)	0.38159(14)	0.37959(11)	0.05168(6)	0.0334(5)
O(1)	0.3946(3)	0.1866(2)	0.21905(13)	0.0317(12)
N(1)	0.3098(3)	0.0645(3)	0.2911(2)	0.0267(12)
N(2)	0.3573(3)	0.2560(3)	0.0787(2)	0.0280(12)
C(11)	0.4257(4)	0.1207(3)	0.1863(2)	0.0250(14)
C(12)	0.4268(4)	0.0352(3)	0.2063(2)	0.0237(14)
C(13)	0.4625(4)	−0.0304(3)	0.1710(2)	0.0293(17)
C(14)	0.4994(5)	−0.0147(3)	0.1181(2)	0.0357(17)
C(15)	0.4970(4)	0.0697(3)	0.0994(2)	0.0283(17)
C(16)	0.4590(4)	0.1373(3)	0.1320(2)	0.0263(17)
C(17)	0.5424(5)	−0.0863(3)	0.0809(2)	0.0390(17)
C(18)	0.4013(4)	0.0128(3)	0.2662(2)	0.0283(16)
C(19)	0.2949(5)	0.0342(4)	0.3495(2)	0.0397(19)
C(21)	0.4842(5)	0.1971(4)	0.3393(2)	0.0447(19)
C(22)	0.2293(5)	0.2626(4)	0.3023(3)	0.053(2)
C(31)	0.3757(4)	0.4489(4)	0.1199(2)	0.055(3)
C(32)	0.2553(6)	0.4009(4)	0.0016(2)	0.058(3)
C(33)	0.5275(5)	0.3738(4)	0.0142(3)	0.063(3)
C(110)	0.2058(4)	0.0496(4)	0.2604(3)	0.045(2)
C(111)	0.4604(4)	0.2277(3)	0.1099(2)	0.0280(17)
C(112)	0.2576(4)	0.2516(4)	0.1151(2)	0.045(2)
C(113)	0.3379(5)	0.1998(4)	0.0294(2)	0.0427(17)

[a] U(eq) = $^1/_3$ of the trace of the orthogonalized **U**.

Table 4. Final Coordinates and Equivalent Isotropic Thermal Parameters of the Non-Hydrogen Atoms for 2e

atom	x	y	z	U_{eq},[a] Å^2
Al(1)	1.19453(10)	0.17654(4)	0.86513(8)	0.0185(3)
Al(2)	0.91802(10)	0.11896(4)	0.59235(8)	0.0197(3)
Al(3)	0.64736(11)	0.03741(5)	0.79631(8)	0.0218(3)
O(1)	0.9936(2)	0.17126(9)	0.73656(16)	0.0156(6)
N(1)	1.2261(3)	0.27074(12)	0.8328(2)	0.0202(8)
N(2)	0.7487(3)	0.12893(12)	0.8258(2)	0.0192(8)
C(1)	0.9099(3)	0.22667(14)	0.7250(2)	0.0159(8)
C(2)	0.7836(3)	0.21824(14)	0.7168(2)	0.0160(9)
C(3)	0.7055(3)	0.27665(14)	0.7014(3)	0.0194(9)
C(4)	0.7498(3)	0.34070(14)	0.6983(3)	0.0184(9)
C(5)	0.8761(3)	0.34660(14)	0.7069(3)	0.0192(9)
C(6)	0.9543(3)	0.28997(14)	0.7180(2)	0.0168(9)
C(7)	0.6667(4)	0.40242(14)	0.6892(3)	0.0262(11)
C(8)	1.0854(3)	0.29597(14)	0.7192(3)	0.0191(9)
C(9)	1.2705(4)	0.31950(16)	0.9286(3)	0.0317(11)
C(10)	1.3458(3)	0.27158(17)	0.8211(3)	0.0336(11)
C(11)	0.7248(3)	0.15046(14)	0.7163(3)	0.0182(9)
C(12)	0.6851(4)	0.17797(15)	0.8603(3)	0.0371(13)
C(13)	0.9100(3)	0.12278(18)	0.9248(3)	0.0360(11)
C(14)	1.3127(3)	0.11399(16)	0.8528(3)	0.0278(11)
C(15)	1.2396(3)	0.18179(17)	1.0185(3)	0.0263(10)
C(16)	1.0199(3)	0.15469(16)	0.5329(3)	0.0266(10)
C(17)	0.9708(4)	0.02664(15)	0.6524(3)	0.0339(11)
C(18)	0.7034(3)	0.14050(16)	0.4787(3)	0.0289(11)
C(19)	0.4378(4)	0.05351(18)	0.6592(3)	0.0407(12)
C(20)	0.6890(4)	0.01895(16)	0.9476(3)	0.0338(11)
C(21)	0.7498(5)	−0.02523(16)	0.7637(4)	0.0444(16)

[a] U(eq) = $^1/_3$ of the trace of the orthogonalized **U**.

ref 21 for **2d**. All calculations were carried out on a DECstation 5000 cluster. Geometrical calculations (including ORTEP plots) were done with PLATON.[22]

Results and Discussion

Syntheses. By reaction of trimethylaluminum with 1, 2, or 3 equiv of $HOC_6H_4(CH_2NMe_2)$-2 (**3**), all three

(19) Cromer, D. T.; Mann, J. B. *Acta Crystallogr., Sect. A* **1968**, *24*, 321.
(20) Cromer, D. T.; Liberman, D. *J. Chem. Phys.* **1970**, *53*, 1891.
(21) Wilson, A. J. C., Ed. *International Tables for Crystallography*; Kluwer Academic Publishers: Dordrecht, The Netherlands, 1992; Vol. C.
(22) Spek, A. L. *Acta Crystallogr., Sect. A* **1990**, *46*, C34.

Scheme 1. Synthesis and Schematic Structures of the Aluminum Complexes of the Mono-*ortho*-Substituted Phenolate 3[a]
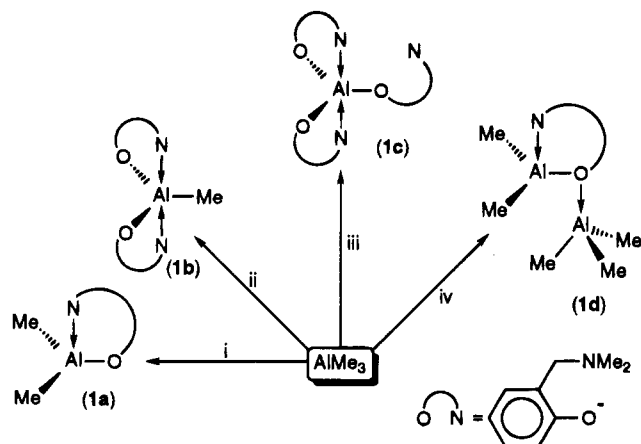
a Key: (i) 1 equiv of $HOC_6H_4(CH_2NMe_2)$-2, hexane, 0 °C; (ii) 2 equiv of $HOC_6H_4(CH_2NMe_2)$-2, hexane, 0 °C; (iii) 3 equiv of $HOC_6H_4(CH_2NMe_2)$-2, hexane, RT; (iv) 0.5 equiv of HOC_6H_4-(CH_2NMe_2)-2, hexane, 0 °C.

Scheme 2. Synthesis and Schematical Structures of the Aluminum Complexes of the Bis-*ortho*-Substituted Phenolate 4[a]
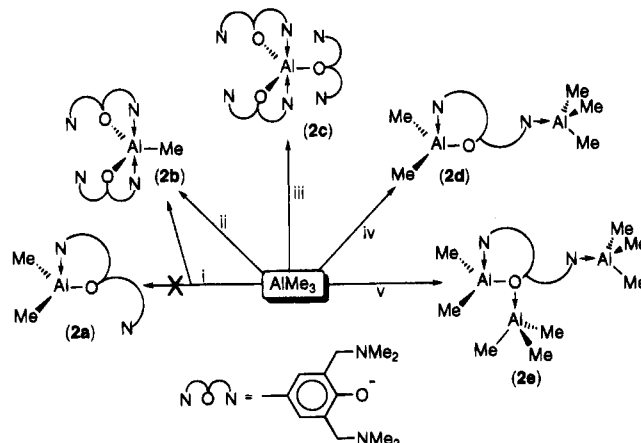
a Key: (i) 1 equiv of $HOC_6H_2(CH_2NMe_2)_2$-2,6-Me-4, hexane, 0 °C; (ii) 2 equiv of $HOC_6H_2(CH_2NMe_2)_2$-2,6-Me-4, hexane, 0 °C; (iii) 3 equiv of $HOC_6H_2(CH_2NMe_2)_2$-2,6-Me-4, hexane, reflux; (iv) 0.5 equiv of $HOC_6H_2(CH_2NMe_2)_2$-2,6-Me-4, hexane, 0 °C; (v) 0.33 equiv of $HOC_6H_2(CH_2NMe_2)_2$-2,6-Me-4, hexane, 0 °C.

substitution products were prepared in high yield (see Scheme 1).

In the case of $HOC_6H_2(CH_2NMe_2)_2$-2,6-Me-4 (4), only the trisubstituted product could be obtained pure and in high yield (see Scheme 2). The disubstituted product was also obtained, but due to its high solubility in both polar and apolar solvents and the fact that it was usually obtained as an oil, we were unable to purify it. The monosubstituted product appeared not to be stable: from the 1:1 reaction of $AlMe_3$ and **4**, AlMe-$(OAr)_2$ and free $AlMe_3$ were obtained in a 1:1 ratio (*vide infra* and Scheme 2).

However, when an excess of $AlMe_3$ was used, the monosubstituted product could be obtained as a Lewis acid–base complex with one or two additional molecules of $AlMe_3$ (see Scheme 2). Similarly, reaction of phenol **3** with an excess of trimethylaluminum afforded a Lewis acid base complex of the mono(phenolate) complex with an additional molecule $AlMe_3$ (see Scheme 1).
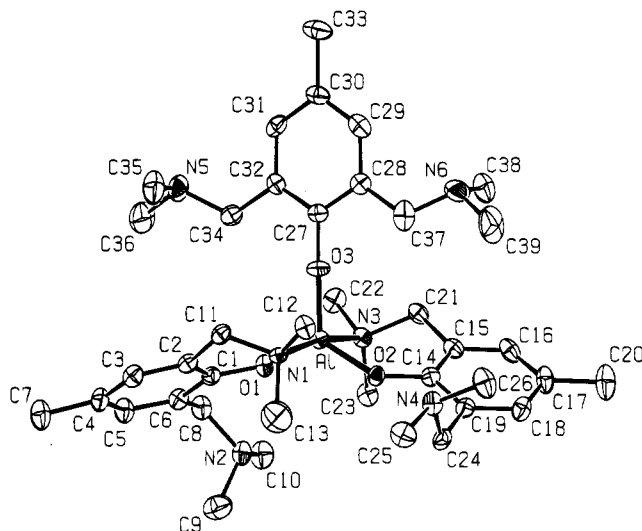

Figure 2. ORTEP representation of $Al\{OC_6H_2(CH_2NMe_2)_2$-2,6-Me-4$\}_3$ (**2c**) with the adopted numbering scheme. Hydrogen atoms have been omitted for clarity.

Table 5. Selected Bond Distances (Å) and Angles (deg) for Complex 2c

Distances			
Al–O(1)	1.754(3)	Al–N(3)	2.074(3)
Al–O(2)	1.764(3)	O(1)–C(1)	1.351(5)
Al–O(3)	1.716(3)	O(2)–C(14)	1.347(5)
Al–N(1)	2.083(3)	O(3)–C(27)	1.336(4)

Angles			
O(1)–Al–O(2)	129.53(13)	O(1)–Al–N(1)	90.10(13)
O(1)–Al–O(3)	114.02(15)	O(1)–Al–N(3)	86.43(13)
O(2)–Al–O(3)	116.43(15)	O(2)–Al–N(1)	86.65(13)
Al–O(1)–C(1)	135.3(2)	O(2)–Al–N(3)	89.09(13)
Al–O(2)–C(14)	133.3(2)	O(3)–Al–N(1)	92.77(13)
Al–O(3)–C(27)	169.8(3)	O(3)–Al–N(3)	96.31(13)
N(1)–Al–N(3)	170.91(13)		

Crystallographic and Spectroscopic Characterization. Selected X-ray structure determinations were carried out for a number of key compounds, which, in combination with spectroscopic data, provided insight into the structural features of these complexes, both in solution and in the solid state. Because of the obvious role that the second *ortho*-CH_2NMe_2 substituent plays in both the instability of the $AlMe_2(OR)$ and the tendency to capture up to two additional $AlMe_3$ molecules by this complex, we concentrated on obtaining X-ray structures of the aluminum phenolate complexes of **4**.

Tris(phenolato)aluminum Complexes. The structure in the solid state of $Al\{OC_6H_2(CH_2NMe_2)_2$-2,6-Me-4$\}_3$ (**2c**) is shown in Figure 2; selected bond distances and angles are given in Table 5. The structure determination reveals the aluminum atom to be surrounded by three phenolate ligands, bonded through oxygen. Two phenolate ligands each have one amino substituent coordinated to the aluminum, while the second one is pendant. In contrast, both amino substituents of the third phenolate ligand are pendant. Accordingly, two of the binding modes shown in Figure 1, *i.e.* *O,N*-bidentate (**c**) and *O*-monodentate (**d**), are present. The geometry around aluminum is slightly distorted trigonal bipyramidal (28% on the Berry pseudorotation path between D_{3h} and C_{4v}), with the three oxygen atoms forming the trigonal plane (the Al is situated 0.007(18) Å out of this plane, $\Sigma(O–Al–O) = 359.98(15)°$); the two coordinating amino substituents occupy the apical posi-

tions ($\angle$ N(1)–Al–N(3) is 170.91(13)°). This geometry around aluminum is general for five-coordinate aluminum complexes containing three normal and two dative bonds.[23] The Al–N distances of the *O,N*-bidentate bonded phenolate ligands are almost equal at 2.083(3) and 2.074(3) Å and lie in the range usually found for amino ligands bound to aluminum (1.957(3)-2.238(4) Å).[8,24-26] The O–Al–O angle involving the oxygen atoms of the two *O,N*-bidentate ligands is larger at 129.53(13)° than the O–Al–O angles involving the oxygen atoms of each of the *O,N*-bidentate ligands and the *O*-monodentate ligand, which are 114.02(15) and 116.43(13)°. This opening of the O–Al–O bond between the two bidentate ligands is probably caused by steric interference between a methyl group of a coordinated amino substituent and the pendant amino substituent on the other bidentate ligand. When this second, pendant substituent is absent, as in the trigonal bipyramidal complex AlMe[O=C(OMe)C$_6$H$_4$-*o*-O]$_2$ (5),[27] bond angles in the trigonal plane are close to 120° (118.28-(10)-120.86(7)°).

The Al–O bond lengths (1.716(3)-1.764(3) Å) are in the range normally found for aluminum phenolates (1,640(5)-1.773(2)°).[5-8] The Al–O bond lengths with the two bidentate, *O,N*-coordinated ligands are in the upper part of this range (1.754(3) and 1.764(3) Å). This is the result of (a) the presence of two coordinating amino substituents, which reduces the Lewis acidity of the metal center, and (b) the formation of the six-membered chelate ring, which pulls the ligand over, leading to relatively small Al–O–C bond angles (135.3-(2) and 133.3(2)°), and reduces the s character in the Al–O bond. Both effects are also present in 5,[27] leading to an Al–O bond length of 1.773(2) Å. As expected, with both amino substituents pendant, the Al–O(3) bond length for the monodentate *O*-bonded ligand is somewhat shorter at 1.716(3) Å and the Al–O(3)–C(27) bond angle is nearly linear (169.8(3)°). This near linear Al–O–C bond angle is most probably a result of steric interference caused by the two pendant amino substituents.

As a result of fluxional processes, the room-temperature ^{1}H NMR spectra of the complexes 2b,c, containing the bis-*ortho*-chelating phenolate ligand, show relatively broad signals that are difficult to interpret. However, the room-temperature ^{13}C NMR spectrum of the tris(phenolate) Al{OC$_6$H$_2$(CH$_2$NMe$_2$)$_2$-2,6-Me-4}$_3$ (2c) contains two signals for both the *ipso*-carbon and the *para*-methyl substituent, both in a 2:1 ratio, which shows that two of the three phenolate ligands are identical. The presence in the ^{1}H NMR spectrum of three separate signals for the benzylic carbon atoms in a 1:1:1 ratio, as well as three separate signals for the aromatic protons, which all integrate for two protons, indicates that there are two ligands with one amino substituent coordinating to the metal center and a pendant one, as well as one ligand of which both substituents are pendant. These observations suggest that the structure found in the solid state for 2c is retained in solution. In

addition, the presence of three separate signals for the aromatic protons at room temperature indicates that rotation of the ligands around the Al–O bond is slow on the NMR time scale at that temperature, which is probably due to a strong Al–N interaction. The analogous complex Al{OC$_6$H$_4$(CH$_2$NMe$_2$)-2}$_3$ (1c), which contains the mono-*ortho*-chelating phenolate ligand 3, shows very similar spectroscopic data. The ^{1}H NMR spectrum of 1c at room temperature shows three signals for the dimethylamino protons of the phenolate ligand. The signals for the benzylic protons consist of one sharp AB pattern, integrating for 2 protons, and one broad AB pattern, integrating for 4 protons. Assuming a trigonal bipyramidal geometry around aluminum (see Scheme 1 and Figure 2), the sharp AB pattern can be assigned to the benzylic protons of the pendant amino substituent and the broad AB pattern to the benzylic protons of the coordinated amino substituents. This view is supported by the ^{13}C NMR spectrum, which shows two signals for the benzylic carbon atoms in a 2:1 ratio, with the most intense at lower field, indicating two coordinated and one pendant amino substituent. This implies that exchange between coordinated and pendant amino substituents is slow on the NMR time scale at room temperature. Heating a toluene-d_8 solution of 1c to 370 K causes coalescence of the benzylic proton signals, which indicates that this process only exists at elevated temperatures. This process most probably involves Al–N bond dissociation/association equilibria.

Bis(phenolato)aluminum Methyl Complexes. The ^{13}C NMR spectrum of the bis(phenolate) AlMe{OC$_6$H$_2$-(CH$_2$NMe$_2$)$_2$-2,6-Me-4}$_2$ (2b) at room temperature shows one signal for the aromatic carbon attached to the oxygen, indicating both phenolate ligands to be identical. The presence of two separate signals for the benzylic carbon atoms shows that one amino substituent of each ligand is coordinated to the aluminum, while the other is not.

For the related bis(phenolate) AlMe{OC$_6$H$_4$(CH$_2$-NMe$_2$)-2}$_2$ (1b) the ^{1}H NMR spectrum at 300 K shows two doublets (AB pattern) for the benzylic protons and a broad signal for the methyl protons. Slight cooling of a toluene-d_8 solution of 1b to 295 K leads to splitting of the signal for the methyl protons into two separate signals ($\Delta G^{\ddagger} = 14.6$ kcal/mol), while raising the temperature to 370 K only leads to sharpening of the signal for the methyl protons. This indicates that on the NMR time scale a fast Al–N dissociation/association process, in combination with inversion of configuration on nitrogen, takes place. The AB pattern for the benzylic protons remains even at 370 K, which suggests a trigonal bipyramidal geometry around aluminum, with the two nitrogen donors in the apical positions and a C_2-axis through the methyl to aluminum bond, as is general for this coordination geometry around aluminum.[23] In this description the two phenolate ligands are equiv, but the benzylic hydrogen atoms diastereotopic (see Scheme 1). For the AB pattern to coalesce, a fast interchange of the positions of the two amino substituents would have to take place. This implies simultaneous dissociation of the Al–N dative bonds and the existence of a three-coordinate intermediate, which is very unlikely. The proposed trigonal bipyramidal geometry is similar to that of the complexes 2c and 1c,
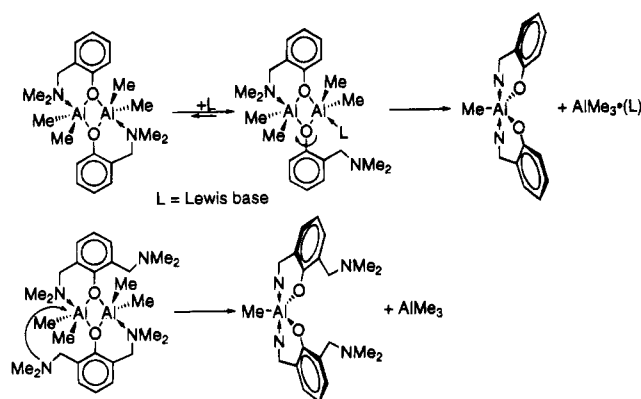
(23) Haaland, A. In *Coordination Chemistry of Aluminum;* Robinson, G. H., Ed.; VCH: New York, 1993; pp 1–51.

(24) Hill, J. B.; Eng, S. J.; Pennington, W. T.; Robinson, G. H. *J. Organomet. Chem.* **1993**, *445*, 11.

(25) Müller, G.; Krüger, C. *Acta Crystallogr., Sect. C* **1984**, *40*, 628.

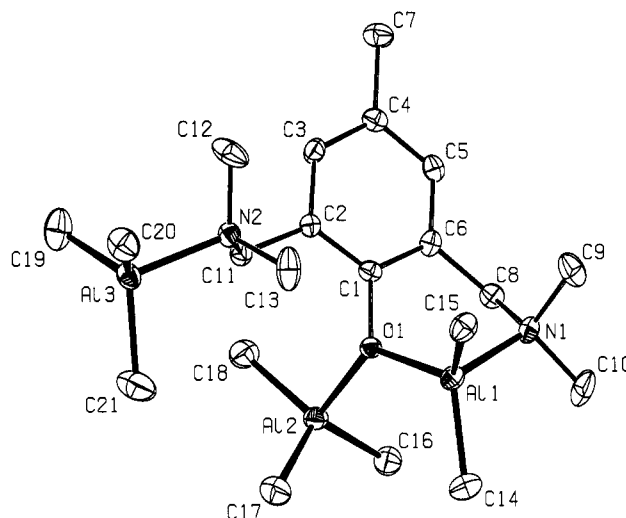(26) Kumar, R.; Sierra, M. L.; Oliver, J. P. *Organometallics* **1994**, *13*, 4285.

(27) Lewiński, J.; Zachara, J.; Mańk, B.; Pasynkiewicz, S. *J. Organomet. Chem.* **1993**, *454*, 5.

Scheme 3. Proposed Mechanism for the Lewis Base induced Ligand Exchange

Figure 3. ORTEP representation of AlMe$_2${OC$_6$H$_2$(CH$_2$-NMe$_2$)$_2$-2,6-Me-4}·N-AlMe$_3$ (**2d**) with the adopted numbering scheme. Hydrogen atoms have been omitted for clarity.

Table 6. Selected Bond Distances (Å) and Angles (deg) for Complex 2d

Distances			
Al(1)−O(1)	1.750(3)	Al(2)−N(2)	2.044(5)
Al(1)−N(1)	1.995(5)	Al(2)−C(31)	1.964(6)
Al(1)−C(21)	1.956(6)	Al(2)−C(32)	1.966(7)
Al(1)−C(22)	1.942(6)	Al(2)−C(33)	1.974(7)
O(1)−C(11)	1.343(6)		

Angles			
O(1)−Al(1)−N(1)	94.80(18)	N(2)−Al(2)−C(31)	104.0(2)
O(1)−Al(1)−C(21)	113.0(2)	N(2)−Al(2)−C(32)	104.0(2)
O(1)−Al(1)−C(22)	111.7(3)	N(2)−Al(2)−C(33)	103.3(2)
N(1)−Al(1)−C(21)	106.0(2)	C(31)−Al(2)−C(32)	113.2(3)
N(1)−Al(1)−C(22)	110.2(2)	C(31)−Al(2)−C(33)	116.1(3)
C(21)−Al(1)−C(22)	118.3(3)	C(32)−Al(2)−C(33)	114.4(3)
Al(1)−O(1)−C(11)	130.5(3)		

the monodentate phenolate ligand being replaced by a methyl substituent.

Mono(phenolato)dimethylaluminum Complexes. The ¹H NMR of the mono(phenolate) AlMe$_2${OC$_6$H$_4$(CH$_2$-NMe$_2$)-2} (**1a**) shows singlets for both the benzylic and methyl protons of the ligand, as well as for the methyl groups on aluminum. This indicates either a monomeric structure, with a four-coordinate aluminum (cf. ref 3), or a dimeric structure with bridging phenolate ligands (cf. ref 1a). In view of the stabilization of monomeric mono(phenolato)aluminum bis(alkyl) complexes by coordination of a Lewis base,[7,8] we assume that **1a** is monomeric.

Attempts to isolate the mono(phenolate) AlMe$_2${OC$_6$H$_2$-(CH$_2$NMe$_2$)-2,6-Me-4} (**2a**) led to disproportionation into the bis(phenolate) **2b** and AlMe$_3$. This ligand exchange may be the result of a Lewis base induced ligand exchange involving the pendant dimethylamino group present.[7] This view is supported by the observation that mono(phenolate) **1a**, which does not contain a pendant dimethylamino group, also disproportionates to give the bis(phenolate) and free AlMe$_3$ upon addition of a Lewis base like THF. In addition, the disproportionation of **2a** is blocked by the presence of a second equiv of AlMe$_3$, and the AlMe$_3$-adduct AlMe$_2${OC$_6$H$_2$(CH$_2$NMe$_2$)-2,6-Me-4}·N-AlMe$_3$ (**2d**) is formed. For this exchange of ligands between two aluminum centers to take place, a transition state has to be formed in which the phenolate ligands bridge between the two aluminum centers (see Scheme 3). The proposed structure for this transition state comprises the geometry found earlier for [ᵗBu$_2$-AlOCH$_2$-2-C$_5$H$_4$N]$_2$,[28] *i.e.* the anionic C- and O-ligand forming the trigonal plane, with the neutral N-donor of the first and the anionic oxygen of the second phenolate ligand occupying the apical positions in a distorted trigonal bipyramidal geometry around each aluminum (see Scheme 3). We propose that the role of the Lewis base in the exchange reaction of **1a** is to make it possible for an amino substituent to dissociate from one aluminum center and, after rotation about the C−O bond of the ligand, make a nucleophilic attack on the other aluminum center, causing a methyl shift and expelling Al(Me)$_3$(L) from the newly formed bis(phenolate). In the case of complex **2a** no rotation of the ligand is necessary, because the pendant amino substituent can make a nucleophilic attack on one aluminum center, while the

other amino substituent dissociates from the other, making the methyl transfer possible (see also Scheme 3). It is interesting to note that in this case the AlMe$_3$ formed during the ligand exchange does not form a Lewis acid−base complex with one of the two pendant amino substituents in **2b**, as is the case in both **2d** and **2e**. This may be due to steric interference.

Trimethylaluminum Adducts of the Mono(phenolato)dimethylaluminum Complexes. The X-ray structure of AlMe$_2${OC$_6$H$_2$(CH$_2$NMe$_2$)$_2$-2,6-Me-4}·N-AlMe$_3$ (**2d**) is shown in Figure 3, and a selection of bond distances and angles are collected in Table 6. The structure contains an AlMe$_2$ moiety and a molecule AlMe$_3$, both bonded to the ligand. The AlMe$_2$ moiety is bonded to the phenolate oxygen, with one of the dimethylamino groups coordinating to the metal center, leading to a distorted tetrahedral geometry around Al-(1). The molecule AlMe$_3$ forms a Lewis acid−base complex with the second, pendant amino substituent, which also results in a distorted tetrahedral geometry around Al(2). Such distorted geometries, with the most acute angles associated with the coordinating Lewis base (N(1) for Al(1) and N(2) for Al(2)), have been observed previously.[7,8] In addition, the geometry around each aluminum atom is very similar to that found for other four-coordinate aluminum phenolates, as is shown by the sum of the angles around Al (excluding those connected with the coordinating Lewis base), which amounts to 343.0(3)° for Al(1) and to 343.7(9)° for Al(2) (literature range: 343.7(6)−346.6(7)°).[7] It is interesting

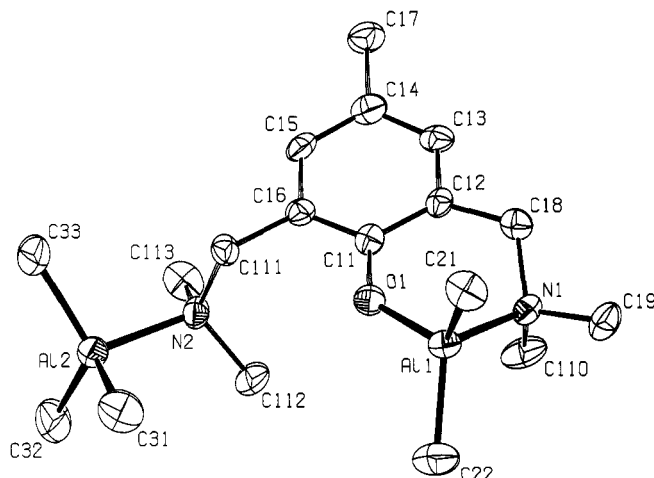(28) van Vliet, M. R. P.; van Koten, G.; de Keijser, M. S.; Vrieze, K. *Organometallics* **1987**, *6*, 1652.

Figure 4. ORTEP representation of $AlMe_2\{OC_6H_2(CH_2\text{-}NMe_2)_2\text{-}2,6\text{-}Me\text{-}4\}\text{-}N\text{-}AlMe_3\cdot O\text{-}AlMe_3$ (**2e**) with the adopted numbering scheme. Hydrogen atoms have been omitted for clarity.

Table 7. Selected Bond Distances (Å) and Angles (deg) for Complex 2e

		Distances		
Al(1)–O(1)	1.855(2)		Al(2)–C(18)	1.979(4)
Al(1)–N(1)	2.021(3)		Al(3)–N(2)	2.059(3)
Al(1)–C(14)	1.939(4)		Al(3)–C(19)	1.968(4)
Al(1)–C(15)	1.954(4)		Al(3)–C(20)	1.975(4)
Al(2)–O(1)	1.989(2)		Al(3)–C(21)	1.974(6)
Al(2)–C(16)	1.984(4)		O(1)–C(1)	1.406(4)
Al(2)–C(17)	1.959(3)			

		Angles		
O(1)–Al(1)–N(1)	96.44(11)		C(17)–Al(2)–C(18)	116.81(18)
O(1)–Al(1)–C(14)	112.21(13)		N(2)–Al(3)–C(19)	104.10(14)
O(1)–Al(1)–C(15)	114.92(16)		N(2)–Al(3)–C(20)	103.00(13)
N(1)–Al(1)–C(14)	109.36(17)		N(2)–Al(3)–C(21)	105.01(19)
N(1)–Al(1)–C(15)	105.10(13)		C(19)–Al(3)–C(20)	116.3(2)
C(14)–Al(1)–C(15)	116.44(16)		C(19)–Al(3)–C(21)	113.61(19)
O(1)–Al(2)–C(16)	106.77(13)		C(20)–Al(3)–C(21)	113.03(18)
O(1)–Al(2)–C(17)	102.23(12)		Al(1)–O(1)–C(1)	114.02(16)
O(1)–Al(2)–C(18)	104.88(14)		Al(2)–O(1)–C(1)	118.20(15)
C(16)–Al(2)–C(17)	115.3(2)		Al(1)–O(1)–Al(2)	122.36(14)
C(16)–Al(2)–C(18)	109.52(16)			

to note that the presence of an intramolecularly coordinating substituent leads to this, generally observed, geometry for four-coordinate aluminum complexes, which illustrates the flexibility of the ligand system. Apparently the coordination geometry is determined by the metal center and not by the rigidity or the spatial arrangement of the O- and two N-donor atom sites of ligand **4**. The Al–O bond length (1.750(3) Å) and the Al–O–C bond angle (130.5(3)°) are comparable to those of Me₂Al(2S,3R)-(+)-4-(dimethylamino)-1,2-diphenyl-3-methyl-2-butanoxide (**6**) (1.726(3) Å and 132.7(3)°, respectively),[26] which also contains a six-membered chelate ring. However, the combination of the Al–O bond length and Al–O–C bond angle in **2d** does not fit the trend observed for other four-coordinate aluminum phenolates $AlR_2(BHT)(L)$ (R = alkyl; BHT = $OC_6H_3^t$-Bu-2,6; L = Lewis base).[8] In these complexes the relatively short Al–O bond lengths, also observed in **2d**, are connected to larger Al–O–C angles, which is described as resulting from π-donation from the oxygen p orbitals to the Al–C and Al–Y σ^* orbitals.[6,8,26,29] The Al–C bond lengths in **2d** are in the range observed previously (1.90–2.01 Å)[5–7,24] but slightly longer around Al(2) (1.964(6)–1.974(7) Å) than around Al(1) (1.942(6) and 1.956(6) Å), as may be expected from the different Lewis acidities of aluminum in $ArOAlMe_2$ vs $AlMe_3$. The same is true for the Al–N dative bond, which is also slightly longer for Al(2) (2.044(5) Å) as compared to Al-(1) (1.995(5) Å). These bond lengths are also in the normal range of 1.957(3)-2.238(4) Å.[6,7,24–26]

The solid state structure of $AlMe_2\{OC_6H_2(CH_2NMe_2)_2$-2,6-Me-4\}-N-AlMe₃·O-AlMe₃ (**2e**) is shown in Figure 4, with selected bond distances and angles collected in Table 7. The structure of this complex is similar to that of **2d**, with an additional molecule of AlMe₃ forming a Lewis acid–base complex with one of the lone pairs on the phenolate oxygen atom. This leads to an almost perfectly trigonal planar surrounded oxygen atom O(1), with the sum of the angles amounting to 354.6(2)° (O(1) is 0.232(2) Å out of the plane defined by Al(1), Al(2),

and C(1)). Compared to the geometry around this oxygen in **2d**, this can be seen as a rehybridization from sp³ to sp², caused by the formation of a Lewis acid–base complex of one of the lone pairs with the AlMe₃ molecule. In accordance with this description, the most acute angles in the distorted tetrahedral geometry around Al(2) are those associated with O(1). The resulting geometry around O(1) is very similar to that found in $Me_2Al(^tBu)N=CHC(Me)_2OAlMe_3$ (**7**),[30] which also contains a bidentate monoanionic N,O-ligand with an additional molecule AlMe₃ coordinated to the oxygen.

The similarity of the coordination geometries of the four-coordinated aluminum atoms in **2e** is shown by the sum of the angles around Al, excluding those connected with the coordinating Lewis base, which amount to 343.6(2)° for Al(1), 341.6(2)° for Al(2), and 342.9(2)° for Al(3). Both the lengthening of the Al(1)–O bond to 1.855(2) Å and the more acute Al(1)–O–C(1) bond angle of 114.02(16)°, as compared to **2d** (1.750(3) Å and 130.5-(3)°, respectively), are to be expected by the coordination of AlMe₃ to the phenolate oxygen and the resulting rehybridization.

In conclusion, the structures found in the solid state for the trimethylaluminum adducts **2d,e** are retained in solution, as observed by NMR spectroscopy. The ¹H NMR of the mono(trimethylaluminum) adduct **2d** shows two separate singlets for both the benzylic and NMe₂ protons, as well as for the methyl groups on aluminum, which integrate for nine (−0.31 ppm) and six (−0.62 ppm) protons, respectively. The AlMe₃ moiety in this complex may form a Lewis acid–base complex with either the amino function or a lone pair on the oxygen in the mono(phenolate). However, on account of the basicity of the amino function and the above mentioned inhibition of the (intramolecular) Lewis base induced ligand exchange, it is to be expected that the AlMe₃ moiety is attached to the second amino substituent and not to the phenolate oxygen, i.e. as found in the crystal structure of **2d** (see Figure 3). The two separate peaks for the AlMe₃ and AlMe₂ moieties remain present even at 80 °C in benzene, so no exchange of methyl groups takes place on the NMR time scale between the two

(29) (a) Barron, A. R.; Dobbs, K. D.; Francl, M. M. *J. Am. Chem. Soc.* **1991**, *113*, 39. (b) Lichtenberger, D. L.; Hogan, R. H.; Healy, M. D.; Barron, A. R. *J. Am. Chem. Soc.* **1990**, *112*, 3369. (c) Lichtenberger, D. L.; Hogan, R. H.; Healy, M. D.; Barron, A. R. *Organometallics* **1991**, *10*, 609.

(30) van Vliet, M. R. P.; van Koten, G.; Rotteveel, M. A.; Schrap, M.; Vrieze, K.; Kojić-Prodić, B.; Spek, A. L.; Duisenberg, A. J. M. *Organometallics* **1986**, *5*, 1389.

aluminum centers. The ^{1}H-NMR of the bis(trimethyl-aluminum) adduct **2e** is similar to that of **2d**, but it shows three singlets for the methyl groups attached to aluminum. These integrate for 9 (-0.26 ppm), 9 (−0.35 ppm), and 6 protons (−0.59 ppm), respectively, corresponding with a Lewis acid−base complex of two separate AlMe₃ moieties with both the pendant amino substituent and a lone pair on the oxygen of the ligand, in accord with the crystal structure (see Figure 4). Here also, the three separate peaks for the methyl groups on the aluminum centers are still present at 80 °C in benzene, indicating that exchange of methyl groups between the aluminum centers does not take place on the NMR time scale. Finally, the ^{1}H NMR spectrum of the mono(phenolate) **1d** shows singlets for both the benzylic and NMe₂ protons, and two separate singlets for methyl groups attached to aluminum, integrating for nine (−0.29 ppm) and six (−0.36 ppm) protons, respectively. A Lewis acid−base complex with a lone pair on the oxygen as found in the crystal structure of **2e** seems likely.

General Properties. With the exception of the bis-(phenolate) **2b**, all complexes are slightly soluble in hexane at room temperature but readily dissolve upon warming, making (re)crystallization from hexane a suitable purification method. They also dissolve readily in aromatic and ethereal solvents, with the exception of the mono(phenolate) **1a**, which undergoes a ligand exchange in the presence of a coordinating solvent (*vide supra*). The bis(phenolate) **2b** is very soluble in apolar, aromatic, and ethereal solvents. This high solubility makes purification of this complex difficult and up to now we have not been able to obtain material sufficiently pure for elemental analyses.

All complexes, except the tris(phenolates) **1c** and **2c**, are air and moisture sensitive due to the presence of an aluminum to methyl bond. Especially the trimethyl-aluminum adducts **1d** and **2d,e** readily burn on exposure to air and react vigorously with moisture.

The AlMe₃-adducts **1d** and **2d,e**, as well as the mono-(phenolate) **1a**, melt without decomposition at relatively low temperatures (90, 125, 115, and 85 °C, respectively), showing the stability of the ligand to metal bonding. The bis(phenolate) **1b** has a melting point higher than 200 °C. In contrast, the tris(phenolate) complexes **1c** and **2c** decompose at 165 and 170 °C, respectively, which may be due to the presence of pendant amino substituents, which introduce additional reactivity, as apparent from the intramolecular Lewis base induced ligand exchange of **2a**.

Both the bis- and tris(phenolates) fail to show interaction with Lewis bases like THF, indicating that the Lewis acidic character of the Al³⁺ ion is strongly reduced by the intramolecular coordination. This is also apparent from the finding that coordination of a third amino substituent to give an octahedral coordination geometry does not occur, as is in principle possible in the complexes **1c** and **2c** (see Figure 2). Such an octahedral geometry around aluminum is found in Al(moz)₃ [Hmoz = 2-(2′-hydroxy-3′-methylphenyl)-2-oxazoline], where all three ligands are bidentate, O,N-bonded.[31]

The relatively facile synthesis of the tris(phenolate) complexes **1c** and **2c** reported here contrasts with the elaborate route used for the synthesis of the first reported aluminum tris(phenolate) complex Al(BHT)₃ (**8**).[5b] The synthesis of the latter complex involved the separation of an equimolar mixture of AlH(BHT)₂ and Li(BHT), formed upon reaction of LiAlH₄ with 3 equiv of (BHT)H, through fractional crystallization. Reaction of AlH(BHT)₂ with an additional 1 equiv of (BHT)H, at reflux temperature in toluene, then afforded **8**. Attempts to synthesize **8** in one step invariably afforded AlR(BHT)₂, even under extreme conditions.[5b] The relatively mild conditions that are sufficient for the syntheses for the tris(phenolate) complexes **1c** and **2c** (room temperature and reflux temperature in hexane, respectively) may be accounted for by (a combination of) two effects. First, the amino substituents present in the phenolate ligands **3** and **4** are less sterically demanding than the *tert*-butyl substituents in BHT. Moreover, in **1c**, each phenolate ligand contains only one *ortho*-amino substituent, leading to considerably less steric congestion. Second, the substitution of the methyl group in the bis(phenolate) complexes **1b** and **2b** may be assisted by coordination of the incoming phenol, *via* an amino substituent, to the aluminum center in the bis(phenolate) complexes. This brings the acidic hydrogen in close proximity to the aluminum to methyl bond.

Conclusions

The crystal structure of **2c** and the structures in solution of the bis- and tris(phenolates) as determined by NMR spectroscopy, show that intramolecular coordination has a positive influence on the stability of monomeric aluminum phenolates. The combination of electronic saturation and steric shielding provided by the *ortho*-amino substituents in **3** and **4** leads to the isolation of aluminum bis- and tris(phenolates), which are monomeric in the solid state, as well as in solution (*vide supra*). Furthermore, the ligands **3** and **4** show great flexibility in their coordination modes, as evidenced by the crystal structures of **2c−e**. For mono-*ortho*-substituted **3**, both bidentate *O,N*-coordination and monodentate *O*-coordination have been observed, while the oxygen in the bidentate mode retains its Lewis basic properties (*cf.* the formation of the AlMe₃-adduct **1d**). For bis-*ortho*-substituted **4**, the second *ortho*-CH₂-NMe₂ substituent can be just an *ortho*-hindering substituent as shown by the solid state structure of **2c** and the structure in solution of both **2c** and **2b**. On the other hand, its Lewis basicity can play a crucial role in the stability of the complexes, as shown by the instability of **2a** and the isolation of **2d** when the Lewis basicity is blocked through a Lewis acid−base complex. Another striking example of this cooperation between anionic and neutral Lewis basic properties is found in the lanthanide phenolate complex Na[Ln{OC₆H₂(CH₂NMe₂)-2,6-Me-4}₃Cl] (Ln = Lu, Y), in which preorganization of the ligand systems, caused by coordination of chloride anion to a neutral lanthanide tris(phenolate), leads to cooperation between pendant amino substituents and the phenolate oxygen atoms to form a six-coordinate cage for the sodium ion.[13]

The similarity of the coordination geometry around the O,N-chelate bonded aluminum centers in **2d,e** (Al-

(31) (a) Hoveyda, H. R.; Karunaratne, V.; Rettig, S. J.; Orvig, C. *Inorg. Chem.* **1992**, *31*, 5408. (b) Hoveyda, H. R.; Rettig, S. J.; Orvig, C. *Inorg. Chem.* **1993**, *32*, 4909. (c) Liu, S.; Rettig, S. J.; Orvig, C. *Inorg. Chem.* **1992**, *31*, 5400.

(1) in both complexes) with that of reported four-coordinate mono(phenolato)aluminum complexes[7] shows the flexibility of the ligand backbone connecting the anionic and neutral Lewis basic sites. This flexibility allows the coordination geometry to be determined by the metal center and not by the interconnectedness of the different binding sites of the ligand. A similar effect is found with respect to the trigonal bipyramidal coordination geometry found for the tris(phenolates) **1c** and **2c**, where electronic saturation of the metal center causes additional potentially intramolecularly coordinating amino substituents to remain pendant where an octahedral geometry with three amino substituents coordinating is in principle possible.[31]

Supporting Information Available: Further details on the structure determinations, including tables of X-ray parameters, atomic coordinates, bond lengths and angles, and thermal parameters for **2c**—**e** (26 pages). Ordering information is given on any current masthead page.

OM950312O